Cytoplasmic Dynein-dependent Vesicular Transport from Early to Late Endosomes

Fernando Aniento, Neil Emans, Gareth Griffiths, and Jean Gruenberg

European Molecular Biology Laboratory, Postfach 10.2209, D-69012 Heidelberg, Germany

Abstract. We have used an in vitro fusion assay to study the mechanisms of transport from early to late endosomes. Our data show that the late endosomes share with the early endosomes a high capacity to undergo homotypic fusion in vitro. However, direct fusion of early with late endosomes does not occur. We have purified vesicles which are intermediates during transport from early to late endosomes in vivo, and analyzed their protein composition in two-dimensional gels. In contrast to either early or late endosomes, these vesicles do not appear to contain unique proteins. Moreover, these vesicles undergo fusion with late endosomes in vitro, but not with each other or back with early endosomes. In vitro, fusion of these endosomal vesicles with late endosomes is stimulated by polymerized microtubules, consistent with the known role of microtubules during early to late endosome transport in vivo. In contrast, homotypic fusion of early or late endosomes is microtubule-independent. Finally, this stimulation by microtubules depends on microtubule-associated proteins and requires the presence of the minus-end directed motor cytoplasmic dynein, but not the plus-end directed motor kinesin, in agreement with the microtubule organization in vivo. Our data strongly suggest that early and late endosomes are separate, highly dynamic organelles, which are connected by a microtubule-dependent vesicular transport step.

CELL-free assays have provided important insights into the mechanisms of biosynthetic and endocytic membrane transport (Balch, 1989; Goda and Pfeffer, 1989; Gruenberg and Clague, 1992; Rothman and Orci, 1992; Schekman, 1992). Early endosomes, in particular, exhibit a high tendency to undergo fusion with each other in vitro (Davey et al., 1985; Gruenberg and Howell, 1986; Braell, 1987; Gruenberg and Howell, 1987; Woodman and Warren, 1988). This process is specific (Gruenberg et al., 1989; Gorvel et al., 1991), dependent on NSF (Diaz et al., 1989), and regulated by protein phosphorylation (Tuomikoski et al., 1989; Thomas et al., 1992; Woodman et al., 1992) as well as GTP-binding proteins (Gorvel et al., 1991; Colombo et al., 1992; Lenhard et al., 1992). This high fusion activity in vitro suggests that early endosomes are highly dynamic in vivo (Gruenberg et al., 1989), as are other compartments involved in membrane transport (Lee and Chen, 1988; Cooper et al., 1990; Hollenbeck and Swanson, 1990). A dynamic endosomal network has, in fact, been observed by video microscopy (Hopkins et al., 1990).

In contrast, relatively little is known about fusion events which may occur between endosomes at later stages of the endocytic pathway. In polarized epithelial MDCK cells the meeting of the apical and basolateral endocytic pathways, which occurs in vivo in late endosomes, has been reconstituted in vitro (Bomsel et al., 1990). However, in nonpolarized cells fusion activity decreases progressively at stages of the pathway beyond early endosomes (Gruenberg and Howell, 1986; Braell, 1987; Gruenberg and Howell, 1987; Woodman and Warren, 1988). In general, the mechanisms of membrane transport between early and late endosomes are unclear and the current views are controversial. One model predicts that early endosomes are formed de novo by the coalescence of plasma membrane-derived vesicles, and then undergo a maturation process, eventually becoming late endosomes (Murphy, 1991; Stoorvogel et al., 1991; Dunn and Maxfield, 1992). A second model proposes that early and late endosomes are stable (preexisting) cellular compartments, connected by transport vesicles (Griffiths and Gruenberg, 1991). Finally, it has been suggested that early and late endosomes are part of a common tubular network (Hopkins et al., 1990).

Whereas the mechanisms of transport remain to be established, it is clear that endocytosed materials are translocated from a peripheral to a perinuclear location, as they progress from early to late endosomes (Hirsch, 1962; Pastan and Willingham, 1981; Herman and Albertini, 1984; Parton et al., 1992*a*) and that this process depends on an intact microtubule network (DeBrabander et al., 1988; Gruenberg et al., 1989; Bomsel et al., 1990). We have observed that after leaving the early endosomes endocytosed markers appear in large (~0.4 μm diam), spherical, multivesicular structures

The current address of Dr. Fernando Aniento and the corresponding address of Dr. Jean Gruenberg is the Department of Biochemistry, University of Geneva Sciences II, 30 quai Ernest Ansermet, 1211-Geneva-4, Switzerland.

before they appear in late endosomes (Gruenberg et al., 1989). When the microtubules are depolymerized, the markers reach these large vesicles, but not the late endosomes. We have proposed that these vesicles mediate the microtubule-dependent passage from peripheral early endosomes to perinuclear late endosomes, and therefore we termed these structures endosomal carrier vesicles (ECVs).[1] Similar vesicles have also been observed as intermediates between early and late endosomes along both the apical and basolateral endocytic pathways in MDCK cells (Bomsel et al., 1990), and along both the axonal and dendritic endocytic pathways in primary hippocampal neurons (Parton et al., 1992*b*).

In the present paper, we have used our in vitro assay to study the mechanisms of transport from early to late endosomes. We show that the late endosomes, as the early endosomes, exhibit a high propensity to undergo homotypic fusion with each other in vitro. Direct fusion of early with late endosomes, however, does not occur. Our in vitro data demonstrate that transport from early to late endosomes involves the fusion of endosomal carrier vesicles with late endosomes. This process, which is specifically stimulated by polymerized microtubules, depends on microtubule-associated proteins and on cytoplasmic dynein, but not kinesin. From these data, we argue that early and late endosomes are highly dynamic but distinct cellular compartments, connected by the microtubule-dependent transport of endosomal carrier vesicles.

Materials and Methods

Cells and Viruses

Monolayers of BHK cells were grown and maintained as described (Gruenberg et al., 1989). For each experiment, a minimum of 6 × 10 cm Petri dishes were plated 16 h before use. Cells were metabolically labeled with 0.2 mCi/dish [^{35}S]Met for 16 h in medium containing 1.5 mg/L Met. To depolymerize microtubules, cells were preincubated with 10 μM nocodazole for 1 h at 37°C, and nocodazole remained present in all incubations up to the internalization step (Gruenberg et al., 1989). Vesicular stomatitis virus (VSV) was produced as described (Gruenberg and Howell, 1985). All manipulations of the cells were at 4°C, except when indicated.

Antibodies

The P5D4 monoclonal antibody against the cytoplasmic domain of the spike glycoprotein G of vesicular stomatitis virus (VSV-G) (Kreis, 1986) was a gift of T. Kreis (University of Geneva, Switzerland), and the 5D3 monoclonal IgM (Vaux et al., 1990) was a gift of S. Fuller (EMBL, Heidelberg, Germany). The SUK4 monoclonal antibody against sea urchin kinesin (Ingold et al., 1988) was a gift of J. M. Scholey (University of California, Davis), and the 70.1 monoclonal IgM against the intermediate chain of chicken cytoplasmic dynein (Steuer et al., 1990) was a gift of M. P. Sheetz (Duke University, Durham, NC).

Fractionation of Endosomes on a Flotation Gradient

We used the same flotation gradient we have previously described (Gorvel et al., 1991; Thomas et al., 1992; Emans et al., 1993). Briefly, cells were homogenized gently to limit damage that may be caused to endosomes, and a post-nuclear supernatant (PNS) was prepared. The PNS was adjusted to 40.6% sucrose, loaded at the bottom of an SW60 tube, and then overlaid sequentially with 16% sucrose in D_2O, 10% sucrose in D_2O, and finally with homogenization buffer (250 mM sucrose, 3 mM imidazole pH = 7.4). The gradient was centrifuged for 60 min at 35,000 rpm using an SW60 rotor. Early endosomes were then collected at the 16%/10% interface and late endosomes at the top of the 10% cushion. Protein determination in the fractions was as described by Bradford (1976).

Immunoisolation of Endosomes

As in our previous studies, we used the cytoplasmic domain of the spike VSV-G as antigen (Gruenberg and Howell, 1985, 1986, 1987; Gruenberg et al., 1989; Thomas et al., 1992; Emans et al., 1993). The G-protein was implanted into the plasma membrane by low pH-mediated fusion of the viral envelope with the plasma membrane. The implanted VSV-G molecules were then internalized essentially as a synchronous wave by incubating the cells at 37°C (Gruenberg and Howell, 1986, 1987). After 45 min in the presence of microtubules, the VSV-G molecules distributed in late endosomes, whereas they remained in endosomal carrier vesicles if microtubules had been depolymerized with 10 μM nocodazole (Gruenberg and Howell, 1989). In either case, the cells were then homogenized and endosomes were separated on the flotation gradient. The fractions containing late endosomes and endosomal carrier vesicles (see Results) were used as input for subsequent immunoisolation. As a solid support, we used, as in our previous studies, anti-mouse Immunobeads (BioRad, Richmond, CA) with bound P5D4 antibody (see Howell et al., 1989 and Gruenberg and Gorvel, 1992).

Endosome Fusion In Vitro

We have used the cell-free assay we have established to reconstitute the occurrence of endosome fusion in vitro (Gruenberg et al., 1989; Tuomikoski et al., 1989; Bomsel et al., 1990; Gorvel et al., 1991; Thomas et al., 1992; Emans et al., 1993). As fusion markers, we used avidin (3.3 mg/ml) and biotinylated HRP (1.8 mg/ml), which were separately internalized by fluid phase endocytosis into two separate cell populations. Avidin distributed into endosomal carrier vesicles after internalization in the absence of microtubules for 10 min at 37°C followed by a 35-min chase in avidin-free medium. Late endosomes were labeled with bHRP under the same conditions, except that microtubules were not depolymerized. Cells were then homogenized, fractionated on the flotation gradient, and the fractions containing bHRP-labeled late endosomes or avidin-labeled carrier vesicles were collected. In the assay, 50 μl of each fraction (~10–15 μg protein) were combined on ice with rat liver cytosol (8 mg protein/ml, final concentration; Aniento et al., 1993) and an ATP-regenerating or -depleting system. The mixture was adjusted to 0.05 mg/ml biotinylated insulin, 60 mM KOAc, 1.5 mM MgOAc, 1 mM DTT and 12.5 mM Hepes, pH 7.4, and incubated for 45 min at 37°C. Then, the avidin-bHRP complex formed upon fusion was extracted in detergent, immunoprecipitated with anti-avidin antibodies, and the enzymatic activity of bHRP was quantified (see Gruenberg and Gorvel, 1992). To calculate the efficiency of fusion, this value was then expressed as a percentage of the total amount of avidin-bHRP complex formed in the presence of detergent and in the absence of biotinylated insulin.

In some experiments, the assay was carried out in the presence of the indicated amounts of exogenous microtubules prepared from purified bovine brain tubulin and stabilized with Taxol (referred to as microtubules in this work), as previously described (Bomsel et al., 1990). Cytosolic MAPs were depleted after polymerization of the endogenous cytosolic tubulin with 20 μM Taxol for 15 min at 37°C, followed by centrifugation at 40,000 *g* for 20 min at 20°C. MAPs were then eluted from the microtubules as described by Scheel and Kreis (1991) and used to recomplement the depleted cytosol in the fusion assay. Heat-stable MAPs from bovine brain and MAPs-depleted cytosol from rat liver were prepared as described by Scheel and Kreis (1991). Photocleavage of cytoplasmic dynein heavy chains was performed as described by Gibbons et al. (1987), Schroer et al. (1989), and Bomsel et al. (1990). Cytosol was depleted of kinesin with the SUK4 monoclonal IgG coupled to Sepharose beads as described by Ingold et al. (1988). Another monoclonal IgG (P5D4) was used as a control antibody. The same procedure was used to deplete cytoplasmic dynein with the 70.1 monoclonal IgM coupled to goat anti-mouse agarose beads, using another monoclonal IgM (5D3) as a control antibody. A 20S fraction enriched in cytoplasmic dynein was prepared after centrifugation of rat liver cytosol in a continuous 5–20% sucrose gradient for 18 h at 35,000 rpm in a SW 40 rotor, as described by Gill et al. (1991).

Two-Dimensional Gel Electrophoresis

A combination of IEF and SDS-PAGE (Celis et al., 1990) was used to re-

1. *Abbreviations used in this paper*: bHRP, biotinylated HRP; ECVs, endosomal carrier vesicles; MAPs, microtubule-associated proteins; PNS, post-nuclear supernatant; VSV, vesicular stomatitis virus; VSV-G, spike glycoprotein G of vesicular stomatitis virus.

solve proteins in two dimensions as described previously (Thomas et al., 1992; Emans et al., 1993).

Electron Microscopy

In our morphological studies of in vitro fusion, the endosomal carrier vesicles and the late endosomes of two cell populations were separately labeled with internalized electron-dense tracers under conditions identical to those used for avidin and bHRP, respectively. For samples embedded in Epon, endosomal carrier vesicles and late endosomes were labeled with HRP and 5-nm BSA-gold, respectively. For cryo-sections, endosomal carrier vesicles and late endosomes were labeled with 5- and 16-nm BSA-gold, respectively. In some in vivo experiments, ECVs and late endosomes (and possibly lysosomes) were labeled with different tracers in the same cells. Then, 16-nm BSA-gold was internalized for 20 min at 37°C and chased for 40 min. The microtubules were then depolymerized by treating the cells for 1 h at 37°C with 10 μM nocodazole. ECVs were subsequently labeled with 5-nm BSA-gold internalized in the presence of nocodazole for 10 min at 37°C, followed by a 30-min chase. Processing for electron microscopy was as previously described (Griffiths et al., 1984, 1989). For quantifying the data shown in Tables III and IV, the structures were sampled in a systematic fashion by moving the grid using translational controls of the electron microscope in fixed directions across the sample. Each structure of interest that was observed was recorded.

Results

Several studies have shown that early endosomes are highly fusogenic in vitro, and that the fusion capacity of endosomes progressively decreases at stages of the endocytic pathway beyond the early endosomes (Davey et al., 1985; Gruenberg and Howell, 1986; Braell, 1987; Gruenberg and Howell, 1987; Diaz et al., 1988; Gruenberg et al., 1989). These experiments, however, could not establish whether late endosomal compartments were indeed fusogenic, albeit to a lesser extent than early endosomes, or whether the observed fusion activity reflected a contamination due to the presence of fusogenic early endosomes. Therefore, our first objective in the present study was to separate late endosomal compartments from early endosomes in order to test their in vitro fusion activity.

Separation of Endosomal Carrier Vesicles and Late Endosomes from Early Endosomes

We showed previously that, using a flotation gradient, early endosomes containing rab5 and labeled 5 min after fluid phase endocytosis of HRP at 37°C, could be separated from late endosomes, containing the cation-independent mannose-6-phosphate receptor, rab7 and labeled with HRP internalized for 10 min at 37°C, and then chased for 35 min in HRP-free medium (Chavrier et al., 1991; Gorvel et al., 1991; Emans et al., 1993). However, our previous studies also indicated that, in the presence of microtubules, internalized tracers appear in ECVs after leaving early endosomes, but before appearing in late endosomes (Gruenberg et al., 1989). To unambiguously determine the position of ECVs in the gradient, we made use of our observations that when the microtubules were depolymerized during the internalization step, markers remained in ECVs and did not reach late endosomes (Gruenberg et al., 1989; Bomsel et al., 1990). The content of ECVs was thus labeled, after microtubule depolymerization, by fluid phase endocytosis of HRP for 10 min at 37°C followed by a 35-min chase in HRP-free medium. After fractionation, HRP was then found in the same fraction as the late endosomes (see also Table II). However, as expected from our previous studies (Gruenberg et al., 1989), an electron microscopy study of the fractions confirmed that internalized markers then localized predominantly to ECVs (which typically contain low amounts of lgp-like proteins, see Figs. 2 and 10 and Table IV) as is the case in vivo (see Fig. 9 and Table III). In contrast, when the microtubules were present internalized markers then reached late endosomes containing high amounts of lgp-like proteins (Figs. 2, 9, and 10 and Table III, IV). Thus, both ECVs and late endosomes could be separated from the highly fusogenic early endosomes using the flotation gradient.

ECVs Undergo Fusion with Late Endosomes In Vitro

Since ECVs appear to be intermediates between early and late endosomes in vivo, we then tested whether ECVs undergo fusion with late endosomes in vitro. To measure fusion we used the in vitro assay we have previously established (Gruenberg et al., 1989; Tuomikoski et al., 1989; Bomsel et al., 1990; Gorvel et al., 1991; Thomas et al., 1992; Emans et al., 1993). ECVs were labeled with avidin, which was internalized, after microtubule depolymerization, for 10 min at 37°C followed by a 35-min chase in avidin-free medium. Late endosomes were labeled after internalization of bHRP using the same pulse-chase conditions, but in the presence of microtubules (Gruenberg et al., 1989). The cells were then homogenized and endosomes were fractionated on the gradient. The fractions containing avidin-labeled ECVs and bHRP-labeled late endosomes were then used in the in vitro assay. If fusion occurs, a product is formed between avidin and bHRP which is then immunoprecipitated with anti-avidin antibodies and the enzymatic activity of bHRP is quantified.

As shown in Fig. 1, fusion of ECVs with late endosomes occurred in the assay. The process was cytosol- and ATP-dependent, sensitive to low concentrations of GTPγS, and inhibited by NEM, like many other membrane transport steps that have been analyzed in vitro (Gruenberg and Clague, 1992; Rothman and Orci, 1992; Schekman, 1992). The efficiency of the process was, however, relatively low ($\sim$10% of the total amount of complex that could be formed in detergent) when compared to early endosome fusion, in agreement with the previously observed decrease in fusion activity at stages of the pathway beyond early endosomes (Gruenberg and Howell, 1989). The fusion assay was then repeated using ECVs and late endosome fractions labeled with HRP and 5-nm BSA-gold, respectively, and the samples were examined by electron microscopy. As shown in Fig. 2, both markers then colocalized in the lumen of vesicles with the typical appearance of BHK late endosomes, which contain large electron-lucent inclusions (Gruenberg et al., 1989). A morphometric study showed that 13% of the gold-labeled profiles also contained the reaction product of HRP, a fusion efficiency consistent with our biochemical quantification. These experiments establish that ECVs undergo fusion with late endosomes in vitro.

The ECV-Late Endosome Fusion Process Is Stimulated by Polymerized Microtubules

An intact microtubule network is required for the passage from ECVs to late endosomes in vivo (Gruenberg et al., 1989). As shown in Fig. 3 *A*, in vitro fusion of ECVs with late endosomes was stimulated more than twofold by the ad-

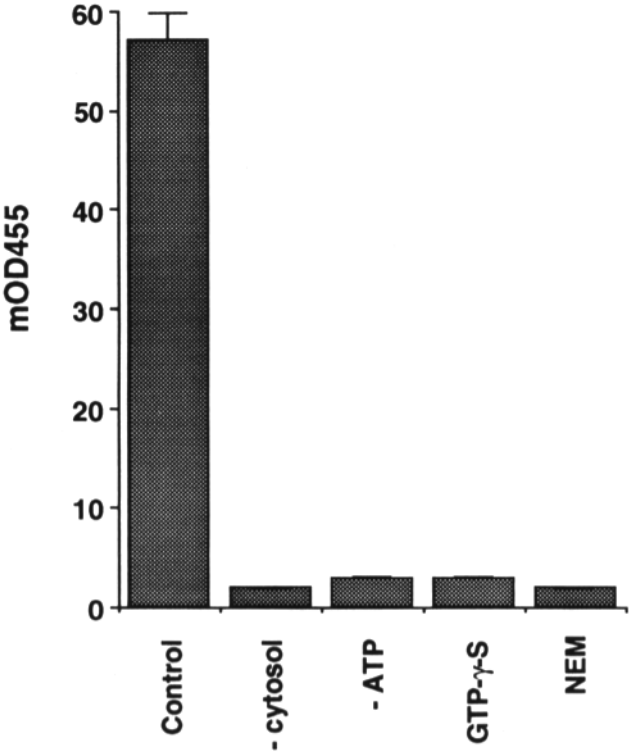

Figure 1. Fusion of endosomal carrier vesicles (*ECVs*) with late endosomes in vitro. An avidin-labeled ECV fraction and a bHRP-labeled late endosome fraction were separately prepared by flotation on a step sucrose gradient. (*Control*) In the fusion assay, both fractions were mixed in the presence of ATP, cytosol, biotinylated insulin and salts, and then incubated for 45 min at 37°C. At the end of the assay, the avidin-bHRP complex formed upon fusion was immunoprecipitated with anti-avidin antibodies, and the enzymatic activity of bHRP was quantified spectrophotometrically at 455 nm (mOD455). (*-ATP*) The assay was in the absence of ATP. (*-cytosol*). The assay was in the absence of cytosol. (*GTPγS*) Cytosol and membranes were pretreated separately with 10 μM GTPγS for 10 min at room temperature, and then used in the cell-free assay. (*NEM*) Cytosol and membranes were mixed together with 1 mM NEM for 15 min on ice, and then NEM was quenched with 1 mM DTT for 15 min on ice. As a control, cytosol and membranes were mixed together with both NEM and DTT for 30 min on ice. Then, fusion occurred with the same efficiency as in the control.

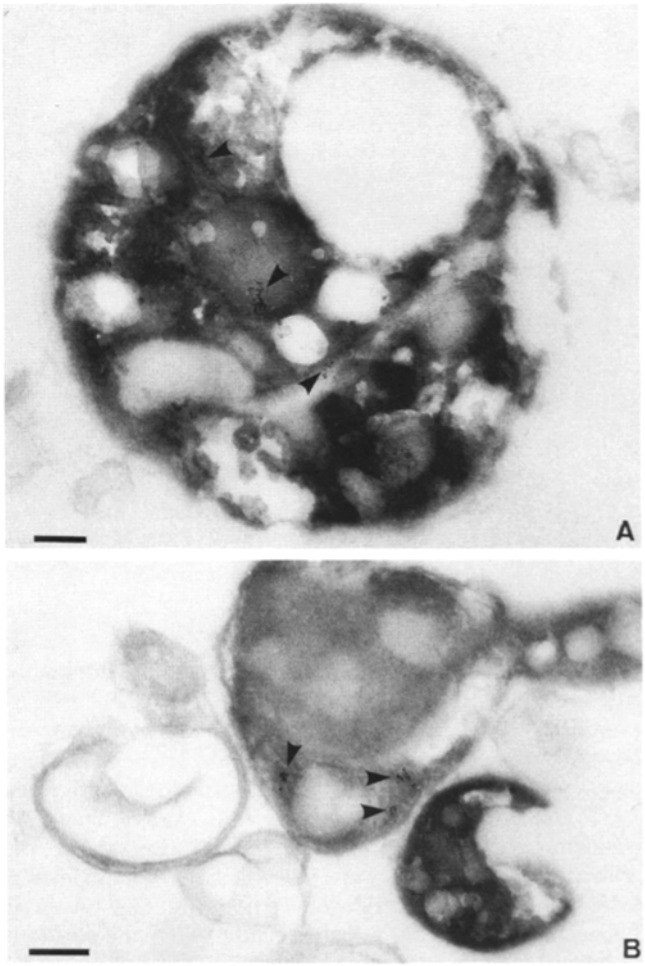

Figure 2. Morphological characterization of ECV-late endosome fusion in vitro. The endosomal carrier vesicles and late endosomes of two cell populations were separately labeled with HRP and 5-nm BSA-gold, using the same conditions as used for avidin and bHRP, respectively (see text). Both endosomal fractions were prepared and used in the cell-free assay as in Fig. 1. Samples were then embedded in Epon and processed for electron microscopy. HRP was revealed cytochemically using diaminobenzidine as a substrate. No colocalization of HRP and 5-nm BSA-gold was observed when the assay was carried out in the absence of ATP. Then, the markers distributed in structures with the typical morphology of ECVs and late endosomes, respectively. However, when the assay was carried out in the presence of ATP, 5-nm BSA-gold particles (*arrowheads*) colocalized with the electron dense reaction product of HRP in the lumen of structures with large internal inclusions typical for BHK late endosomes, and the efficiency of the process was 13%. The structure shown in the right bottom corner of *B* resembles an ECV, which did not undergo fusion: no gold particles are seen in this section plane and the structure appears darker, presumably because its HRP content has not been diluted into the larger late endosome volume. Bar, 0.1 μm.

dition of 5 μg microtubules prepared from purified bovine brain tubulin and stabilized with Taxol. This amount is within the range of the endogenous cytosolic tubulin present in the assay. In fact, Taxol-mediated polymerization of the endogenous tubulin also stimulated fusion, although to a lesser extent. The microtubule-dependent stimulation was ATP-sensitive (not shown) and inhibited by 10 μM GTPγS. Stimulation of ECV-late endosome fusion thus resulted in a fusion efficiency ~23%, a value comparable to the efficiency of early endosome fusion.

Late Endosomes Undergo Homotypic Fusion with Each Other in a Microtubule-independent Manner

Next we investigated whether other endosome fusion events may also be reconstituted in vitro. We tested all possible combinations of fractions prepared after avidin and bHRP internalization into early endosomes, ECVs, or late endosomes. As expected (Gruenberg and Howell, 1986; Braell, 1987; Gruenberg and Howell, 1987; Diaz et al., 1988; Gruenberg et al., 1989), the homotypic fusion of early endosomes was the most efficient endosome fusion event and was not stimulated by microtubules (Fig. 4). These experiments

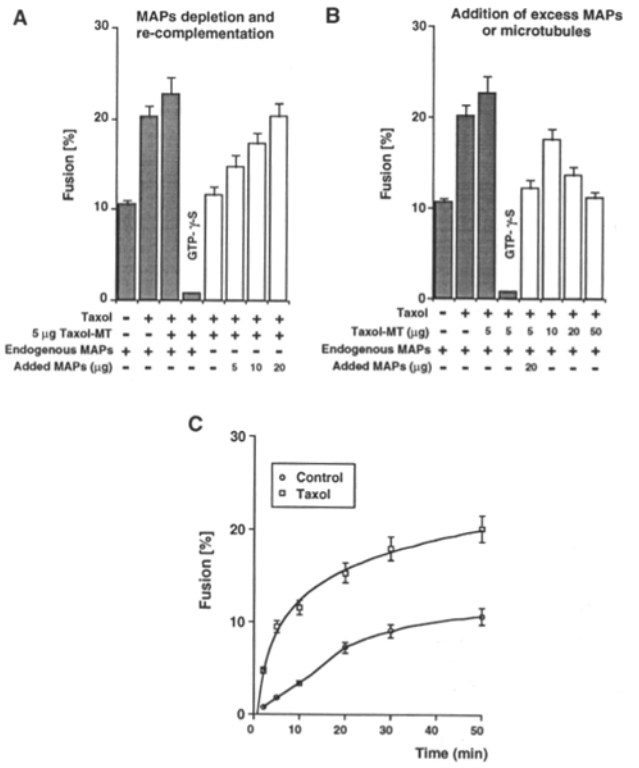

Figure 3. Stimulation of ECV-late endosome fusion in vitro by microtubules and MAPs dependence of the process. ECVs and late endosome fractions, labeled with avidin and bHRP, respectively, were prepared and used in the in vitro assay as in Fig. 1. (*A*) Shaded bard indicate control experiments carried out in complete cytosol containing endogenous MAPs, either without Taxol addition, or after polymerization of endogenous tubulin with 20 μM Taxol, or after further addition of 5 μg Taxol-stabilized bovine brain microtubules, or under the latter conditions plus 10 μM GTPγS (*GTPγS*). Open bars indicate experiments carried out in the presence of 5 μg Taxol-microtubules (as above) but after depletion of the MAPs from the cytosol by affinity binding to microtubules. This depleted cytosol was either used directly in the assay or recomplemented with the indicated amounts of MAPs (5–20 μg) eluted from microtubules after the affinity-binding step. (*B*) Shaded bars correspond to the same conditions as in *A*. Open bars indicate experiments carried out either in the presence of 5 μg Taxol microtubules but after addition of 20 μg excess MAPs prepared either from bovine brain or from rat liver cytosol, or without MAPs addition but in the presence of increasing amounts of microtubules. (*C*) Conditions were as in *A*, except that the fusion assay was carried out for different times, as indicated, in the absence (*control: open circles*) or in the presence of 20 μM Taxol (*Taxol: open squares*).

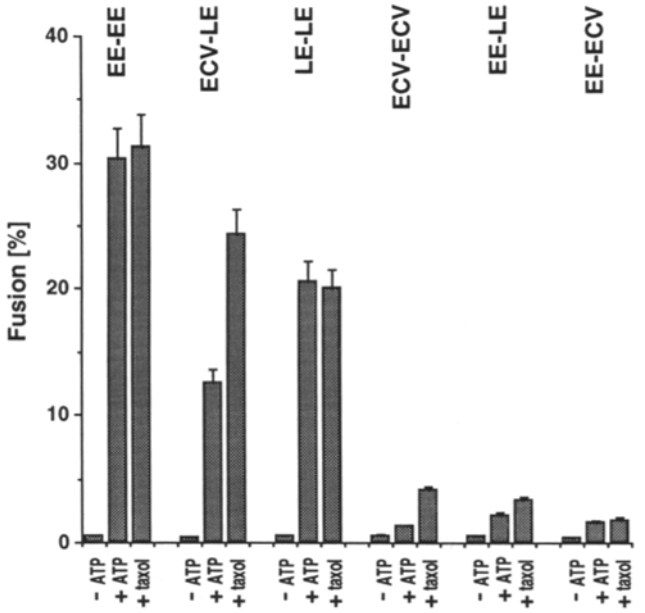

Figure 4. Fusion of different endosomes in vitro. Early endosomal fractions (*EE*) were prepared from two cell populations after separate internalization of avidin or bHRP for 5 min at 37°C. ECV and late endosome (*LE*) fractions, labeled with avidin or bHRP, were prepared as described (see text). The combinations of different fractions in the assay are indicated. To allow better comparisons between experiments, all fractions were always prepared in parallel during the same day, and used in the assay at the same protein concentrations (10–12 μg of fraction per point) using the same cytosol preparation. The assay was as in Figs. 1–3, with (*+ATP*) or without (*−ATP*) ATP in the absence of polymerized microtubules, or with ATP after polymerization of endogenous tubulin with 20 μM Taxol (*+Taxol*).

also showed that late endosomes shared with early endosomes the capacity to undergo homotypic fusion with each other, and that this process was also microtubule-independent (Fig. 4). Among these different fusion events, only the fusion of ECVs with late endosomes could be stimulated by polymerized microtubules (see also Fig. 3). All three fusion events were specific since early endosomes did not fuse directly with late endosomes nor with ECVs (Fig. 4). In addition, ECVs did not undergo homotypic fusion with each other, in contrast to early or late endosomes (Fig. 4).

These experiments show that ECV-late endosome fusion exhibits properties which are different from both homotypic fusion events with respect to the stimulatory role of microtubules. Since early endosomes do not fuse directly with late endosomes and ECVs do not fuse with each other or with early endosomes, these experiments strongly suggest that transport from early to late endosomes in vivo occurs via the fusion of ECVs with late endosomes.

Kinetics of ECV-Late Endosome Fusion in the Presence of Microtubules and Microtubule-associated Proteins Dependence of the Process

We then further characterized the process of microtubule-mediated stimulation during ECV-late endosome fusion. Fig. 3 *A* shows that microtubule-associated proteins (MAPs) are required, since stimulation was almost completely abolished after MAPs depletion and almost completely restored after MAPs recomplementation. However, addition of MAPs in excess inhibited stimulation (Fig. 3 *B*), without interfering with the fusion in the absence of microtubules (not shown). This effect is likely to reflect a competition of MAPs for vesicle-binding sites on the microtubules since a similar effect has been observed for the in vitro binding of ECVs (Scheel and Kreis, 1991) or exocytic vesicles (Van der Sluijs et al., 1990) to microtubules. Finally, excess microtubules also reduced stimulation (Fig. 3 *B*), presumably because of a dispersion of the vesicles on different microtubules or because some factors then became limiting.

A kinetic analysis of the time course of in vitro fusion

Table I. The ECV-Late Endosome Interactions Depend on Cytoplasmic Dynein But Not Kinesin

	Stimulation (*fold*)	Inhibition of stimulation (%)
Control without MT	1.00 ± 0.15 (15)	-
Control with MT	1.98 ± 0.15 (15)	-
Kinesin depletion		
Control antibody (P5D4)	1.95 ± 0.15 (6)	3
Specific antibody (SUK4)	1.82 ± 0.14 (6)	16
Cytoplasmic dynein depletion and recomplementation		
UV-photocleavage ctrl (+ NE)	1.96 ± 0.15 (3)	2
UV-photocleavage	1.33 ± 0.05 (3)	66
UV-photocl. + cyt. dynein	1.71 ± 0.05 (2)	27
Control antibody (5D3 IgM)	1.89 ± 0.10 (2)	9
Specific antibody (70.1 IgM)	1.23 ± 0.04 (2)	77

Fusion of ECVs and late endosomes was measured as described in the text. Unless indicated, all experiments were carried out in the presence of 20 μM Taxol to promote the polymerization of endogenous cytosolic tubulin (See Fig. 3). Kinesin was immunodepleted using the SUK4 antibody; the control IgG was the P5D4 antibody. Cytoplasmic dynein was cleaved by UV light in the presence of vanadate, and then vanadate was quenched with 5 mM norepinephrin (UV-photocleavage). In the control, the UV-treatment was in the presence of norepinephrin (UV-photocl. ctrl, +NE); and then, no photocleavage of cytoplasmic dynein was observed on SDS-gels (not shown). After UV-mediated photocleavage of endogenous cytoplasmic dynein, the assay was recomplemented with a 20S fraction enriched in cytoplasmic dynein prepared from rat liver (UV-photocl. + cyt. dynein). Alternatively, cytoplasmic dynein was immunodepleted using the 70.1 IgM; the control IgM was the 5D3 antibody. The fold stimulation mediated by microtubules is indicated (≈2X), fusion without microtubules being normalized to 1.0. Inhibition of microtubule-mediated stimulation is expressed as a percentage of the difference between the values obtained with microtubules (≈2X) and without microtubules (1.0). Values are mean ± SD. The number of experiments is indicated in parentheses.

showed that stimulation by microtubules followed a hyperbolic profile, whereas fusion in the absence of microtubules increased linearly at early time points and then reached a plateau (Fig. 3 *C*). Microtubule-mediated stimulation was maximal during the first 10 min of the reaction, corresponding to a 4–5-fold increase. Altogether these observations demonstrate that encounters between ECVs and late endosomes, which both interact with microtubules in vivo, are facilitated by microtubules in vitro, thereby increasing the extent of fusion.

The ECV-Late Endosome Interactions Depend on Cytoplasmic Dynein But Not Kinesin

Since microtubules stimulated ECV-late endosome fusion in a MAPs-dependent manner, we tested whether motor proteins were involved in this process. Two types of motors have been characterized which move vesicles toward opposite ends of microtubules in vitro, cytoplasmic dynein (Paschal et al., 1987), a minus-end directed motor (Schroer et al., 1989), and kinesin (Vale et al., 1985), a plus-end directed motor (Schroer et al., 1988). As shown in Table I, depletion of cytosolic kinesin with the SUK4 anti-kinesin antibody (Fig. 5 *D*) did not have a significant effect. In contrast, depletion of cytoplasmic dynein, either by UV-mediated photocleavage of its heavy chain (Fig. 5, *A–B*) or by immunodepletion with the 70.1 anti-dynein antibody (Fig. 5 *C*), produced a significant inhibition of the microtubule-dependent stimulation of fusion (66 and 77%, respectively;

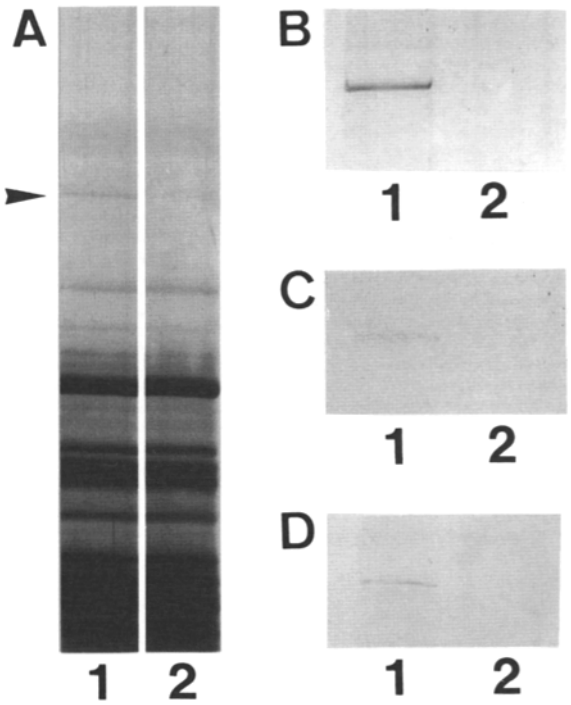

Figure 5. Gel electrophoresis of cytoplasmic dynein and kinesin. (*A*) Cytoplasmic dynein was photocleaved after treating rat liver cytosol with UV light in the presence of 100 μM vanadate and 2 mM ATP. The samples were electrophoresed in 4% acrylamide gels, and the gels were silver-stained. One band at the mobility of cytoplasmic dynein heavy chain (*arrowhead*, ≈360 kD) was significantly reduced (lane *2*) when compared with control cytosol (lane *1*), and presumably reflected the photocleavage of cytoplasmic dynein. The abundance of the protein was too low to detect unambiguously the lower molecular weight cleavage products in a region of the gel containing many other polypeptides. Photocleavage did not occur in the presence of 5 mM norepinephrin (not shown). (*B*) Control and photocleaved cytosols were immunoprecipitated with the 70.1 antibody, the samples were electrophoresed in 4% acrylamide gels, and the gels were silver-stained. Lane *1* shows cytoplasmic dynein heavy chain in the control cytosol, which is almost undetectable after photocleavage (lane *2*). (*C*) Cytoplasmic dynein from rat liver cytosol was immunodepleted with the 70.1 IgM (lane *2*) or with a control IgM (5D3) (lane *1*) and analyzed by gel electrophoresis followed by Western blotting with the 70.1 antibody. (*D*) Kinesin from rat liver cytosol was immunodepleted with the SUK4 IgG (lane *2*) or with a control IgG (P5D4) (lane *1*) and analyzed by gel electrophoresis followed by Western blotting with the SUK4 antibody. Only the relevant parts of gels and immunoblots are shown.

Table I). Moreover, microtubule-dependent stimulation could then be restored to a significant extent by addition of a 20S fraction containing cytoplasmic dynein (Table I). These observations indicate that the interactions of ECV and/or late endosomes with microtubules are facilitated by the motor protein cytoplasmic dynein, but not by kinesin, in agreement with the minus-end directed movement of endosomes towards the pericentriolar region in non-polarized cells (Pastan and Willingham, 1981; Matteoni and Kreis, 1987; DeBrabander et al., 1988).

Table II. Fractionation of Endosomes

	Yield (%)	Enrichment (*fold*)
Endosomal carrier vesicles	11	136
Late endosomes	11	142

As antigen for immunoisolation, we used the cytoplasmic domain of the VSV-G protein, originally implanted into the plasma membrane. To label endosomal carrier vesicles, implanted G molecules were cointernalized at 37°C, in the absence of microtubules, with HRP, a marker of the endosomal content, for 10 min followed by a 35-min chase in HRP-free medium. Late endosomes, and possibly lysosomes, were labeled with G molecules and HRP under the same internalization conditions but in the presence of microtubules. The corresponding endosomal compartments were then fractionated on a gradient (Gorvel et al., 1991) followed by immunoisolation with antibodies against VSV-G cytoplasmic domain (see Gruenberg and Gorvel, 1992). The enzymatic activity of HRP present in the fractions was quantified. Yields are expressed as a percentage of the amounts present in the homogenate. The final enrichment over the homogenate was calculated from the relative specific activities for the gradient (18 X), and from the enrichment over a control without the specific antibody for immunoisolation (8X) (Howell et al., 1989). We used gentle homogenization conditions to limit damage to endosomes; as a result ≈30% of the cell remained intact and ≈50% of HRP was lost in the nuclear pellet.

ECVs and Late Endosomes Differ in Their General Protein Composition and in Their lgp Content

To further characterize ECVs and late endosomes, we analyzed their protein composition. An additional purification step was then required since both compartments cofractionated on the gradient. Fractions were prepared as above from cells that had been metabolically labeled to equilibrium with [^{35}S]Met and the corresponding endosomal compartment, ECVs or late endosomes, was retrieved by immunoisolation (Howell et al., 1989; Gruenberg and Gorvel, 1992 and references therein). Using internalized HRP as a marker of the endosomal content, both ECVs and late endosomes could be separately enriched more than 100 ×, with a yield of ~11% over the homogenate (Table II).

The fractions were then analyzed in high resolution 2D gels. The protein patterns of ECVs and late endosomes are shown in Figs. 6 *A* and 7 *A*, respectively. As controls, the immunoisolation step was carried out in parallel with a nonrelevant antibody and the corresponding gels are shown in Figs. 6 *B* and 7 *B*. All proteins that could be detected in the controls were disregarded in our analysis. The ECV fraction contained ~30 major proteins, whereas the pattern of late endosomal protein was more complex, accounting for ~50 major species. Most of the ECV proteins were detected in the late endosome fraction. However, the latter fraction contained proteins that were not detected in ECVs or were present in very low amounts, even after overloading the gel with ECVs or after longer exposures of the same gels (data not shown). These included in particular very acidic proteins (pI ≤ 5.0) with a migration pattern reflecting presumably different glycosylation states (Fig. 7 *A*, *arrowheads*).

Two of these acidic glycoproteins of 120 and 45 kD were identified with specific monoclonal antibodies, termed 4a1 and 2a5, respectively (Fig. 8). Both antigens were abundant in late endosomes (Figs. 7 *A* and 8), but present in low amounts in early endosomes (Fig. 8) and ECVs (Fig. 6 *A*). This distribution was confirmed by immunogold labeling of cryosections. As shown in Fig. 9, both antibodies labeled predominantly the limiting membrane of late endosomes and lysosomes. Low level of labeling was seen on the plasma membrane and early endosomes (not shown). Both antigens thus share the hallmarks of lysosomal glycoproteins (lgps) (Kornfeld and Mellman, 1989), being acidic, presumably glycosylated, proteins present in low amounts on the plasma membrane and early endosomes, but very abundant in late endosomes and lysosomes. To distinguish unambiguously between ECVs and late endosomes, these were labeled with electron-dense tracers endocytosed in the absence or in the presence of microtubules, respectively. As shown in Fig. 9 and quantified in Table III, both antigens were present in low amounts in ECVs, when compared to late endosomes. These experiments indicate that ECVs and late endosomes differ in their general protein composition and in their lgp content, and that ECVs, in contrast to late endosomes, do not appear to contain unique proteins.

In Vivo Transfer to lgp-rich Late Endosomes

Since ECVs and late endosomes differ in their lgp content, we used the 4a1 and 2a5 antibodies as markers of the fusion process in the electron microscope. In these experiments, the fusion assay was carried out in the presence of microtubules exactly as described above, except that ECVs and late endosomes were labeled with 5 and 16 nm BSA-gold, respectively (see Table III), instead of avidin and bHRP. Cryosections were then processed for immunogold labeling with the 4a1 and 2a5 antibodies.

When the fractions were mixed under conditions where fusion did not occur (in the absence of ATP), the bulk of the 5-nm BSA-gold particles remained within structures with the typical appearance of ECVs and containing low levels of 4a1 and 2a5 (Fig. 10 *D*, Table IV), while most of the structures containing 16-nm BSA-gold were heavily labeled with the 4a1 and 2a5 antibodies (Fig. 10 *E*, Table IV). Essentially no colocalization of the two gold particles within the same vesicular profile could be observed (Table IV). As expected, this distribution was identical to that observed in vivo after internalization under the same conditions (Table III). When the fusion was allowed to proceed in the presence of ATP, however, colocalization of the 5- and 16-nm BSA-gold particles occurred with an efficiency comparable to that measured biochemically (Table IV). Then, both types of gold particles were almost exclusively detected within structures with the appearance of late endosomes containing high amounts of the 4a1 and 2a5 antigens (Table IV and Fig. 10). These experiments demonstrate that upon fusion the markers present in ECVs, which contain low amounts of lgps, are transferred to late endosomes, containing high amounts of lgps.

Discussion

We have studied three distinct endosome fusion events in vitro, and characterized the corresponding compartments by subcellular fractionation and morphology. Our data show that both early and late endosomes share the capacity to undergo homotypic fusion in vitro, but that fusion of early with late endosomes does not occur. Further, ECVs, which are intermediates between early and late endosomes in vivo, undergo fusion with late endosomes in vitro. ECV-late endosome interactions are facilitated by microtubules and depend on the minus-end directed motor cytoplasmic dynein, consistent with the retrograde direction of endosome movement in vivo. From these data, we argue that early and late endo-

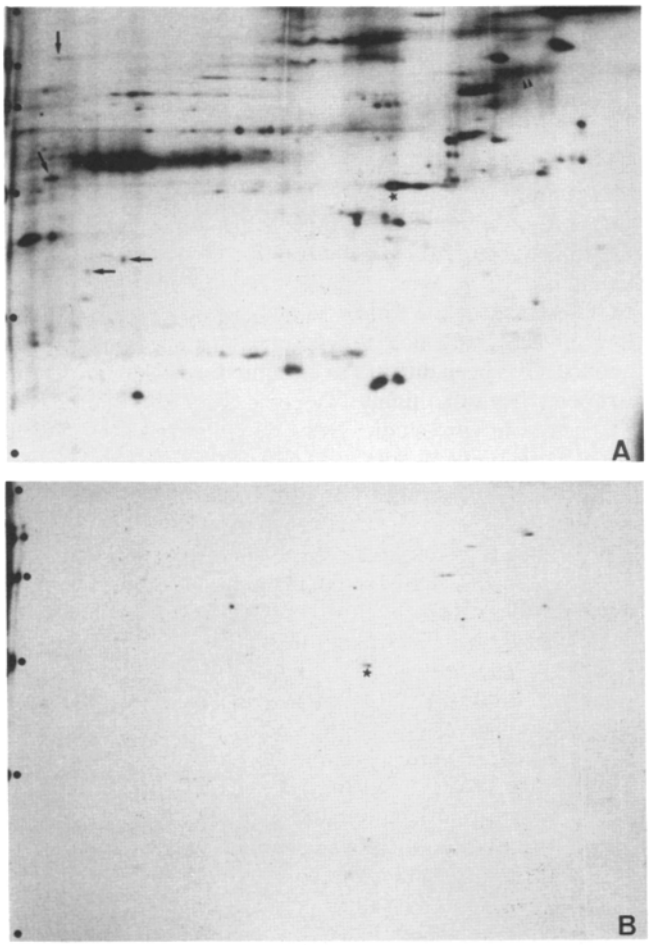

Figure 6. Protein composition of ECVs. (*A*) Purified ECV fractions (≈20 μg) were prepared from cells metabolically labeled to equilibrium with [^{35}S]Met, by combining a flotation gradient with immunoisolation. The fractions were analyzed by isoelectrical focusing in the first dimension (direction of electrophoresis from left to right and pH gradient linear from 4.5 to 7.4), followed by SDS-PAGE in the second dimension (direction of electrophoresis from top to bottom), and then autoradiography. The arrows point at examples of proteins which are present both in ECVs and late endosomes (see Fig. 7 *A*), and which are also found in early endosomes (Emans et al., 1993). The star shows the position of actin, identified by its mobility in 2D gels. The double arrowheads point at an acidic protein also present in late endosomes (see Fig. 7 *A*). Molecular weight markers are indicated (14.3, 30, 46, 69, 97, and 200 kD). (*B*) Same as *A*, but the specific antibody was omitted during immunoisolation. The pH gradient in the gel was linear between 4.5 and 7.4.

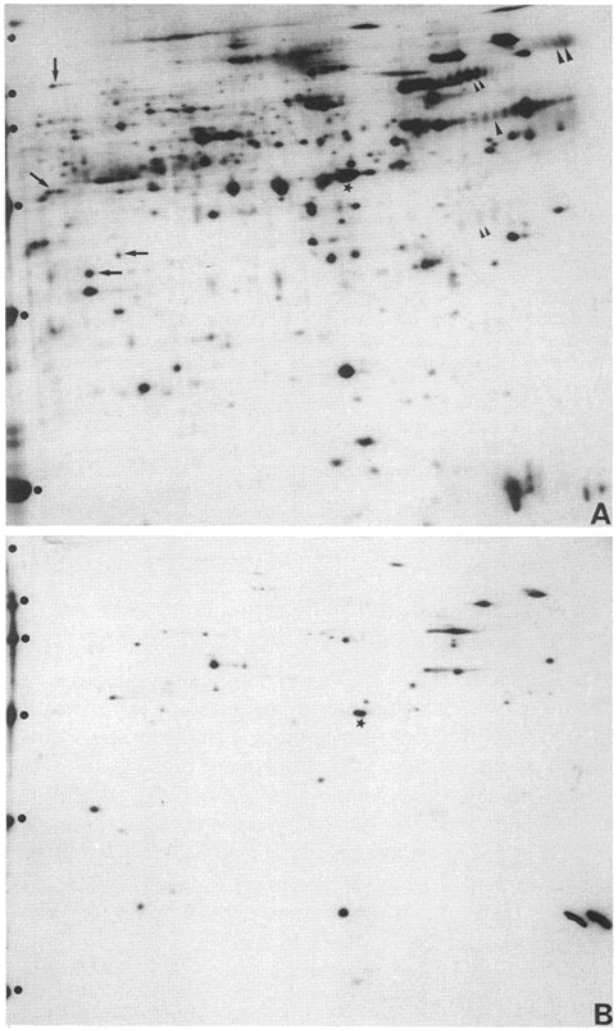

Figure 7. Protein composition of late endosomes. (*A*) A purified late endosome fraction (≈20 μg) was prepared from cells metabolically labeled to equilibrium with [^{35}S]Met, by combining a flotation gradient with immunoisolation. The fractions were analyzed by 2D gel electrophoresis followed by autoradiography, as in Fig. 6. The arrows point at the same proteins as in Fig. 6, and the star shows the position of actin. Arrowheads indicate examples of acidic proteins, which are presumably glycosylated and abundant in late endosomes. Double large arrowheads point at the 4al (120 kD) antigen and a single large arrowhead points at the 2a5 (45 kD) antigen (see Fig. 8), which are both lgp-like proteins. Molecular weight markers are as in Fig. 6. (*B*) Same as *A*, but the specific antibody was omitted during immunoisolation.

somes are highly dynamic but distinct cellular compartments connected by the microtubule-dependent transport of endosomal carrier vesicles.

Homotypic Fusion of Early Endosomes and Late Endosomes

It is now well established that early endosomes exhibit a high tendency to undergo homotypic fusion with each other in vitro; several components regulating this process have been identified (for a review see Gruenberg and Clague, 1992). We have interpreted this high fusion capacity as an indication that individual elements of the early endosome may be connected by fusion and fission events in vivo, forming a dynamic network. Recent studies have shown that overexpression of the small GTPase rab5, which stimulates early endosome fusion in vitro (Gorvel et al., 1991) and endocytosis in vivo (Bucci et al., 1992), causes the formation of large early endosomal structures (Bucci et al., 1992). In contrast, overexpression of a rab5 mutant with a single point mutation in the GTP-binding domain, which inhibits early endosome fusion in vitro (Gorvel et al., 1991) and endocytosis in vivo (Bucci et al., 1992), leads to the fragmentation of early endosomes into small vesicles (Bucci et al., 1992; Parton et al., 1992*b*).

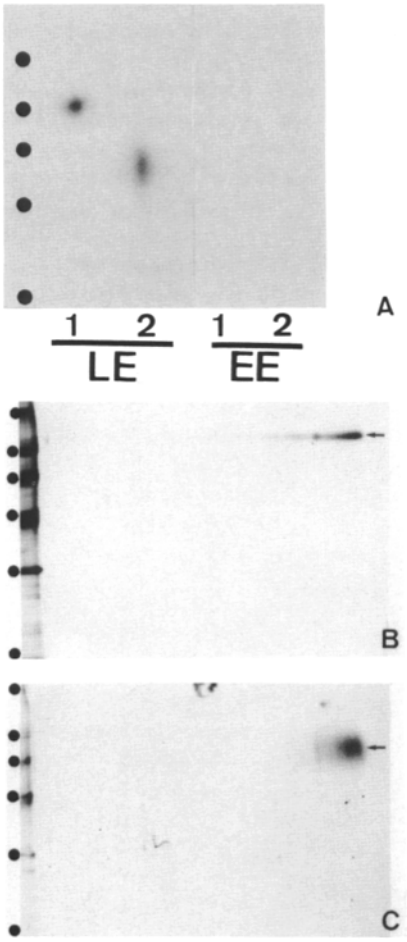

Figure 8. Characterization of the 4a1 and 2a5 antigens. (*A*) Early (*EE*) and late (*LE*) endosomal fractions were prepared from metabolically labeled cells (see Figs. 6–7) using a flotation gradient. The 4a1 (lane *1*; 120 kD) or 2a5 (lane *2*; 45 kD) antigen was then immunoprecipitated with the corresponding antibody from equivalent amounts of proteins from either fraction, and analyzed by SDS-PAGE. Molecular weight markers are as in Fig. 6. (*B*) The same experiment as in *A* was repeated from a late endosomal fraction using the 4a1 antibody, and the immunoprecipitate was analyzed in 2D gels. Molecular weight markers are as in Fig. 6. (*C*) Same as *B* with the 2a5 antibody.

Our present data demonstrate that late endosomes also exhibit a propensity to undergo homotypic fusion with each other in vitro, suggesting that late endosomes may also be highly dynamic in vivo. In macrophages, a dynamic network of tubular lysosomes radiating from the pericentriolar region has been extensively described (Phaire-Washington et al., 1980; Swanson et al., 1987; Hollenbeck and Swanson, 1990). These structures were recently shown to exhibit characteristics typical of late endosomes (Rabinowitz et al., 1992) since they contain both the small GTPase rab7 (Chavrier et al., 1990) and the mannose-6-phosphate receptor (Griffiths et al., 1988). Interspecies cell fusion experiments have also shown that both late endosomes and lysosomes are highly dynamic in vivo (Deng and Storrie, 1988; Deng et al., 1991). The fact that early and late endosomes share the capacity to undergo homotypic fusion in vitro and may form dynamic networks in vivo, supports the view that both endosomal compartments are highly plastic organelles, as are other compartments involved in membrane transport, including the endoplasmic reticulum (Lee and Chen, 1988) and *trans*-Golgi elements (Cooper et al., 1990).

In Vitro Fusion of Endosomal Carrier Vesicles with Late Endosomes

The mechanisms of membrane transport from early to late endosomes have been controversial. Until now, in vitro studies of membrane transport in non-polarized cells have not provided major new insights into this question, in part because it has been difficult to separate late endosomal compartments from the highly fusogenic early endosomes.

However, in vitro studies using the polarized MDCK cell have shown that apically and basolaterally derived endosomes undergo fusion presumably with common late endosomes (Bomsel et al., 1990), where both pathways meet in vivo (Bomsel et al., 1989; Parton et al., 1989). However, the precise sequence of fusion events leading to this in vitro meeting process could not be established, because no attempt was made in these experiments to separate early from late endosomes, nor apical from basolateral endosomes.

Our approach was to make use of our previous observations that markers internalized in BHK cells appear sequentially in early endosomes, in large and spherical multivesicular structures, and then in late endosomes (Gruenberg et al., 1989). Since the markers reached these large vesicles but not the late endosomes after microtubule depolymerization, we proposed that these intermediate vesicles function as ECVs transported on microtubules. Similar intermediate structures were observed both during apical and basolateral endocytosis in MDCK cells (Bomsel et al., 1990) and during axonal and dendritic endocytosis in cultured primary neurons (Parton et al., 1992*a*). Using a gradient that we had established (Chavrier et al., 1991; Gorvel et al., 1991; Emans et al., 1993), we have separated both ECVs and late endosomes from the highly fusogenic early endosomes.

Our data demonstrate that ECVs undergo fusion with late endosomes in vitro. An electron microscopy analysis shows that markers originally present in ECVs are delivered upon fusion to typical late endosomes, which contain high amounts of two lgp-like proteins (4a1 and 2a5); purified late endosomes indeed contain high amounts of these two proteins, in contrast to ECVs, when analyzed in 2D gels. The process of ECV-late endosome fusion is specific since ECVs do not fuse with each other in a homotypic manner, in contrast to early or late endosomes, and since ECVs do not undergo fusion with early endosomes. Like other steps of membrane transport (Balch, 1992; Gruenberg and Clague, 1992; Pfeffer, 1992), this fusion event is inhibited by low concentrations of GTPγS, indicating that GTP-binding proteins regulate this process. This fusion event is also inhibited by NEM, suggesting that NSF (Rothman and Orci, 1992) or another NEM-sensitive factor (Goda and Pfeffer, 1991) is required. Finally, this process is different at the molecular level from homotypic endosome fusion events, since ECV-late endosome interactions are facilitated by microtubules and depend on MAPs and cytoplasmic dynein.

Microtubules and Motors

The stimulatory role of microtubules during ECV-late endo-

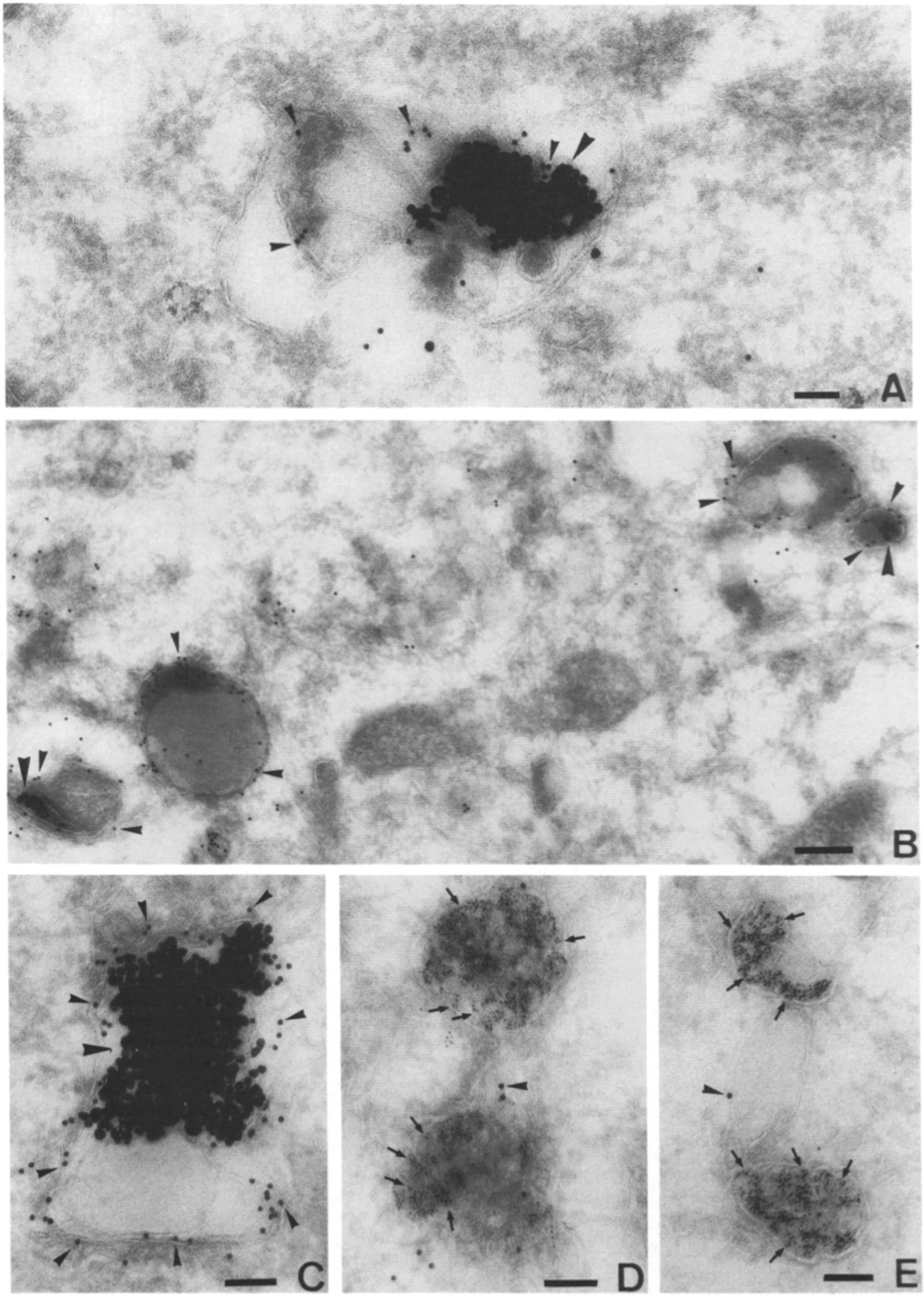
A
B
C
D
E

Table III. The 4a1 and 2a5 Antigens Are Not Abundant in Endosomal Carrier Vesicles

	Negative [%]		Positive [%]	
	4a1	2a5	4a1	2a5
ECVs: 5 nm gold internal. without MT	69 [11]	86 [18]	31 [5]	14 [3]
LEs: 16 nm gold internal. with MT	4 [1]	17 [5]	96 [23]	83 [24]

To label late endosomes, and possibly lysosomes, 16-nm BSA-gold was internalized for 20 min at 37°C, and then chased for 40 min (LEs). The microtubules were then depolymerized by treating the cells for 1 h at 37°C with 10 μM nocodazole. ECVs were subsequently labeled with 5-nm BSA-gold internalized for 10 min at 37°C and chased for 35 min in the presence of nocodazole. It is unlikely that this relatively short second incubation without microtubules significantly changed the distribution of the 16-nm BSA-gold particles internalized into late endosomes; even after several hours of chase, late endosomes remain heavily labeled with gold particles (Griffiths et al., 1990). Cryosections were prepared, labeled with 4a1 or 2a5, and the bound antibodies were revealed with 9-nm proteinA-gold. With the 2a5 antibody, we classify structures containing very low amounts of antigen (less than two 9-nm gold particles per profile) as being negative, and to those containing high amounts (more than two gold particles) as being positive. Since the extent of labeling with the 4a1 antibody was far higher (see Fig. 9), the threshold was then set at four gold particles per profile. The number of counted profiles is in parentheses and the percentages are indicated.

some fusion is very likely to reflect endosome-microtubule interactions and movement, since the process depends on MAPs and the motor protein cytoplasmic dynein. Although microtubules may not be polarized by centrioles in our assay, in contrast to the intracellular situation, they can form large interconnected networks (unpublished). Our preliminary experiments by differential interference contrast microscopy suggest that ECVs can bind to and move on these networks in vitro. The simplest interpretation is, therefore, that ECV-late endosome fusion is stimulated by microtubules in the assay because vesicle movement on microtubules facilitates the encounters between vesicles destined to fuse. The hyperbolic kinetics of fusion in the presence of microtubules, when compared to the linear profile observed in their absence, supports this interpretation. From these data, it is not clear whether both ECVs and late endosomes can move on microtubules in vitro. However, we have observed no stimu-

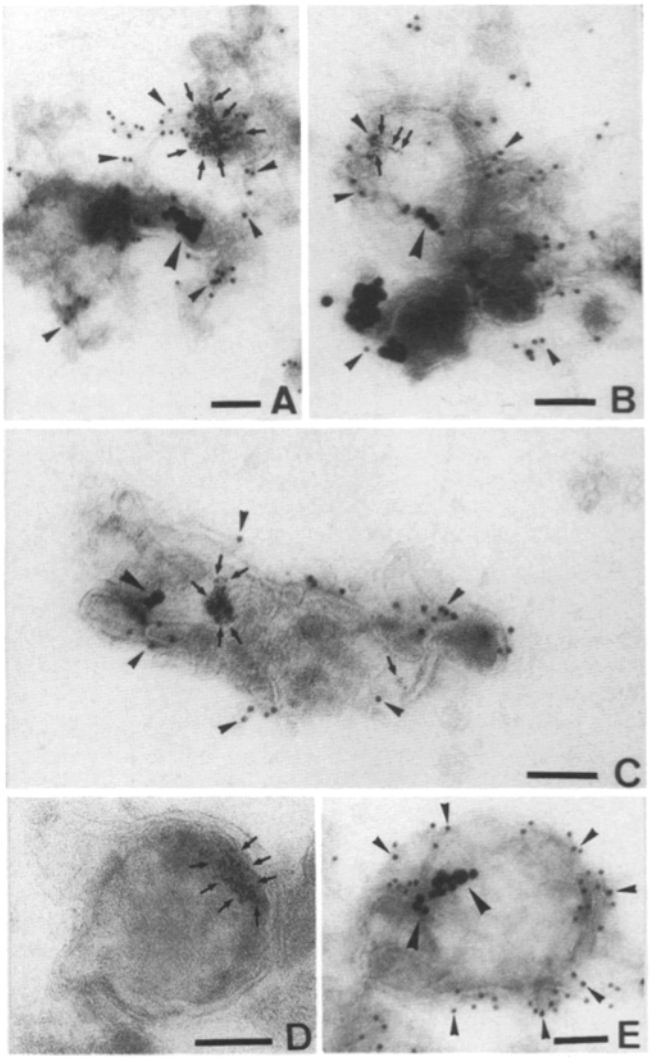

Figure 10. Transfer of markers to lgp-rich late endosomes upon ECV-late endosome fusion in vitro. ECV and late endosome fractions were separately prepared from two cell populations after internalization of 5-nm BSA-gold (*small arrows*) or 16-nm BSA-gold (*large arrowheads*), respectively, using the same conditions of internalization as in Fig. 1. The fractions were then used in the assay in the presence of 20 μM Taxol (see Fig. 3). At the end of the assay, samples were fixed, cryo-sectioned, and the sections were labeled with the 4a1 antibody (*small arrowheads*) as in Fig. 9. (*A–C*) The pictures illustrate the colocalization of 5 and 16-nm BSA-gold particles in the lumen of 4a1-positive late endosomes, when fusion was allowed to occur in the presence of ATP. (*D–E*) When the assay was carried out in the absence of ATP, almost no colocalization of 5 and 16-nm gold particles within the same profiles could be observed. Then, the 5-nm gold particles were found in structures with the typical morphology of ECVs with very low amounts of 4a1 (*D*), while 16-nm gold particles were found in structures with the typical morphology of late endosomes and heavily labeled with 4a1 (*E*) (see also Table IV for quantitation). Bar, 0.1 μm.

Figure 9. Sub-cellular distribution of 4a1 and 2a5 antigens. Late endosomes (and possibly lysosomes), as well as ECVs were labeled in the same cells with different tracers. To label late endosomes (and possibly lysosomes), 16-nm BSA-gold (*large arrowheads*) was internalized for 20 min at 37°C, and then chased for 40 min. Cells were then treated for 60 min at 37°C with 10 μM nocodazole, to depolymerize the microtubules. Then, ECVs were labeled with 5 nm BSA-gold (*small arrows*) internalized for 10 min at 37°C, and then chased for 30 min in the presence of 10 μM nocodazole. Thawed cryo sections were prepared after fixation and the sections were labeled either with 4a1 or 2a5. Either antibody was revealed with 9-nm Protein A-gold (*small arrowheads*). (*A*) Colocalization of 2a5 with 16-nm gold in a late endosome or a lysosome. (*B–C*) Colocalization of 4a1 with 16 nm gold in a late endosome or a lysosome. Note that the extent of labeling is much higher with 4a1 than with 2a5. (*D–E*) Comparatively low amounts of 4a1 (*D*) or 2a5 (*E*) (*small arrowheads*) are observed in ECVs, identified by their spherical appearance and by their content of 5 nm BSA-gold (*small arrows*). Bar: (*A*, *C*, *D*, and *E*) 0.1 μm; Bar: (*B*) 0.2 μm.

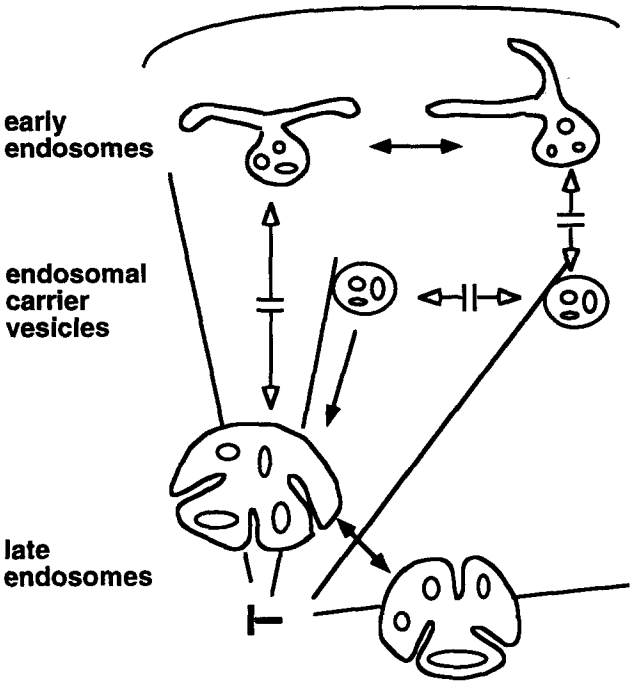

Figure 11. Outline of endosome fusion events in vitro. The different fusion events reconstituted in vitro (indicated by *arrows*) are the homotypic fusion of early and late endosomes and the heterotypic fusion of ECVs with late endosomes. Only the latter step is stimulated by microtubules, and this simulation depends on the motor protein cytoplasmic dynein. Broken arrows indicate interactions between endosomes which do not occur in our assay, including fusion of early with late endosomes, homotypic fusion of ECVs, or fusion of ECVs with early endosomes. ECVs form from early endosomes, in a process which requires an active vacuolar ATPase (see note added in proof).

lation by microtubules during the homotypic fusion of late endosomes, suggesting that these may bind to microtubules, but may not move to any significant extent in our assay. Indeed, late endosomes can bind to microtubules in vitro (Bomsel et al., 1990), and are clustered in the perinuclear region in a microtubule-dependent manner in vivo (Matteoni and Kreis, 1987; DeBrabander et al., 1988). Microtubule-binding may be mediated by proteins related to CLIP170 (Pierre et al., 1992).

The effects of microtubules on ECV-late endosome interactions in vitro are likely to reflect their role in vivo, since transport from ECV to late endosomes requires intact microtubules (Gruenberg et al., 1989). In non-polarized cells, microtubules radiate from the microtubule-organizing center in the nuclear region, with their plus-ends pointing towards the cell periphery (Vale, 1987). We find that ECV-late endosome interactions depend predominantly on the minus-end directed motor cytoplasmic dynein (Schroer et al., 1989). This requirement is consistent with the minus-end direction of endosomal vesicle movement from the cell periphery, where early endosomes are found, to the perinuclear region, where late endosomes are clustered (Matteoni and Kreis, 1987; DeBrabander et al., 1988). In epithelial MDCK cells the situation is different. Microtubules are organized longitudinally to the long axis of the cells, with their plus- and minus-ends pointing at the basolateral and apical surfaces, respectively (Bacallao et al., 1989). We found that the meeting of the apical and basolateral endocytic pathways in late endosomes requires intact microtubules in vivo (Bomsel et al., 1990). In vitro, this process is stimulated by microtubules and requires both cytoplasmic dynein and kinesin, suggesting that cytoplasmic dynein may be used for retrograde movement along the basolateral pathway and kinesin for anterograde movement along the apical pathway.

Protein Composition

Our data strongly suggest that transport from early to late endosomes occurs via the fusion of ECVs with late endosomes since early endosomes do not fuse directly with late endosomes and since ECVs do not exhibit homotypic fusion properties (see outline Fig. 11). In addition, an analysis of the protein composition of ECVs and late endosomes in 2D gels shows that essentially all ECV proteins are also present in late endosomes. However, the pattern of late endosomal proteins is more complex, and contains in particular significant amounts of two lgp-like proteins which also localize predominantly to late endosomes and lysosomes on cryosections. It has been argued that because of their abundance, lgps must be the major constituents of the late endosome and lysosome membranes (Kornfeld and Mellman, 1989). A high degree of glycosylation may protect them from the degradative milieu, explaining their slow turn-over rates. Clearly the level of immunogold labeling we observe with either protein is well within the range of lgp 120 in NRK cells (Griffiths et al., 1988, 1990). In addition, a morphological analysis demonstrates that markers originally present in ECVs colocalize with both late endosomal markers and these two lgp-like proteins after fusion. It is highly unlikely that the lgp-like proteins were delivered from the biosynthetic pathway during the short incubation time of our assay, since lgps are long-lived proteins (Kornfeld and Mellman, 1989), and since we detect only very low levels of labeling with the corresponding antibodies in the Golgi stack. The simplest interpretation is, therefore, that ECVs undergo fusion with late endosomes, which contain high amounts of both proteins.

We have previously analyzed the protein composition of purified early endosomes in 2D gels (Emans et al., 1993). Their overall protein composition is significantly different from those of ECVs or late endosomes. Early endosomes, but not ECVs or late endosomes, contain in their 2D patterns annexin II and the small GTPase rab5, which both localize to early endosomes (Chavrier et al., 1990; Emans et al., 1993). Conversely, lgp-like proteins, which are abundant in late endosomes, are not detected or are present in very low amounts amongst early endosomal proteins (Emans et al., 1993). Finally, early endosomes, like late endosomes, appear to have a more complex protein composition than ECVs. In particular, early endosomes, but not ECVs and late endosomes, as expected, contain several proteins that recycle with the cell surface, where they can be biotinylated (Schrotz, P., and J. Gruenberg, unpublished results).

Table IV. Fusion of ECVs with Late Endosomes: Morphometric Quantitation

	Endosomal structures				Fusion [%]		
	Negative [%]		Positive [%]		16 nm gold-positive profiles containing both 5 nm gold and		
	4a1	2a5	4a1	2a5	4a1	or	2a5
Without ATP							
ECVs: 5 nm gold internal. without MT	71 [20]	100 [12]	28 [8]	0 [0]			
LEs: 16 nm gold internal. with MT	23 [3]	17 [3]	77 [10]	83 [14]			
Colocalization: 5 + 16 nm gold [within the same vesicular profile]	−[0]	−[0]	−[1]	−[0]	−[1]		−[0]
With ATP							
ECVs: 5 nm gold internal. without MT	5 [1]	63 [10]	95 [18]	37 [6]			
LEs: 16 nm gold internal. with MT	0 [0]	6 [1]	100 [16]	93 [14]			
Colocalization: 5 + 16 nm gold [within the same vesicular profile]	0 [0]	0 [0]	100 [10]	100 [10]	38 [10/26]		41 [10/24]

Endosomal carrier vesicles (*ECVs*) or late endosomes (*LEs*), were labeled with 5-nm BSA-gold or 16-nm BSA-gold internalized separately into two cell populations under the same conditions as used in the fusion assay for avidin or bHRP, respectively (see legend Fig. 1). The corresponding fractions were then prepared and used in the fusion assay in the presence of microtubules and with or without ATP (as in Figs. 1–3). At the end of the assay, samples were processed for immunogold labeling using thawed cryosections as in Table III, and the percentage of endosomal structures containing either the 4a1 or the 2a5 antigen was calculated as in Table III (number of profiles indicated in parentheses). The differences between the percentages of 2a5- and 4a1-positive structures reflects the differences in the labeling efficiency with these antibodies (see also Table III and Fig. 9). The occurrence of fusion was measured by the colocalization of 5- and 16-nm gold within the same vesicular profiles and is calculated as the percentage of structures containing the late endosome marker (16-nm BSA-gold), which also contained 5-nm BSA-gold originally present in ECVs. All structures containing both gold particles were also positive for either antigen (4a1+ or 2a5+). Fusion efficiency may be underestimated, since many structures containing 5-nm BSA-gold particles became heavily labeled with 4a1 and 2a5 after incubation in the presence of ATP, but contained no 16-nm gold particles in the section plane.

Conclusions

Altogether, our observations show that both early and late endosomes contain unique proteins and undergo homotypic fusion in vitro in a microtubule-independent manner. In contrast, ECVs do not appear to contain major proteins which are unique, suggesting that they are transient components of the endocytic pathway. Moreover, they do not undergo homotypic fusion in vitro, but they fuse with late endosomes in a process which is stimulated by microtubules and depends on cytoplasmic dynein. We find it difficult to reconcile these observations with the view that ECVs undergo a maturation process and become late endosomes (Murphy, 1991; Stoorvogel et al., 1991; Dunn and Maxfield, 1992). Our observations rather suggest that both early and late endosomes are highly dynamic and distinct organelles. ECVs, after being formed from early endosomes at the cell periphery (Gruenberg et al., 1989), are transported on microtubules towards the perinuclear region via the activity of the minus-end directed motor cytoplasmic dynein, and eventually fuse with late endosomes.

We are particularly grateful to Carmen Walter and Heike Wilhelm for their expert technical assistance, particularly with the 2D gels; to Hege Hardersen, for her dedication in the preparation of monoclonal antibodies; and to Heinz Horstmann for his expert technical assistance with the electron microscopy. We are also grateful to Michael Sheetz for providing us with antibodies against cytoplasmic dynein, and to Jonathan Scholey for giving us antibodies against kinesin. We also thank Rob Parton, Bernard Hoflack, and Steve Pfeiffer for their helpful suggestions and for critically reading the manuscript.

F. Aniento was a recipient of an Alexander-von-Humboldt fellowship.

Received for publication 17 June 1993 and in revised form 13 September 1993.

Note Added in Proof. In support of the view presented in this paper (see outline Fig. 11), we have recently obtained evidence that endosomal carrier vesicles (which are competent to fuse with late endosomes in vitro) form from early endosomes in a process that requires an active vacuolar ATPase (Clague, M. J., S. Urbé, F. Aniento, and J. Gruenberg. 1993). Vacuolar ATPase activity is required for endosomal carrier vesicle formation. In press.

References

Aniento, F., E. Roche, A. Cuervo, and E. Knecht. 1993. Uptake and degradation of glyceraldehyde-3-phosphate dehydrogenase by rat liver lysosomes. *J. Biol. Chem.* 268:10463–10470.

Bacallao, R., C. Antony, C. Dotti, E. Karsenti, E. H. Stelzer, and K. Simons. 1989. The sub-cellular organization of Madin-Darby canine kidney cells during the formation of a polarized epithelium. *J. Cell Biol.* 109:2817–2832.

Balch, W. E. 1989. Biochemistry of interorganelle transport. *J. Biol. Chem.* 264:16965–16968.

Balch, W. E. 1992. From G minor to G major. *Current Biology.* 2:157–160.

Bomsel, M., R. G. Parton, S. A. Kuznetsov, T. A. Schroer, and J. Gruenberg. 1990. Microtubule and motor dependent fusion in vitro between apical and

basolateral endocytic vesicles from MDCK cells. *Cell.* 62:719–731.
Bomsel, M., K. Prydz, R. G. Parton, J. Gruenberg, and K. Simons. 1989. Endocytosis in filter-grown Madin-Darby canine kidney cells. *J. Cell Biol.* 109:3243–3258.
Bradford, M. M. 1976. A rapid and sensitive method for the quantitation of microgram quantities of protein utilizing the principle of protein-dye binding. *Anal. Biochem.* 72:248–254.
Braell, W. A. 1987. Fusion between endocytic vesicles in a cell-free system. *Proc. Natl. Acad. Sci. USA.* 84:1137–1141.
Bucci, C., R. G. Parton, I. H. Mather, H. Stunnenberg, K. Simons, B. Hoflack, and M. Zerial. 1992. The small GTP-ase rab5 functions as a regulatory factor in the early endocytic pathway. *Cell.* 70:715–728.
Celis, J. E., B. Gesser, H. H. Rasmussen, P. Madsen, H. Leffers, K. Dejgaard, B. Honore, E. Olsen, G. Ratz, J. B. Lauridsen, B. Basse, S. Mouritzen, M. Hellerup, A. Andersen, E. Walbum, A. Celis, G. Bauw, M. Puype, J. vanDamme, and J. Vanderckhove. 1990. Comprehensive two-dimensional gel protein databases offer a global approach to the analysis of human cells: the transformed amnion cells (AMA) master database and its link to genome DNA sequence data. *Electrophoresis.* 11:989–1071.
Chavrier, P., J.-P. Gorvel, E. Stelzer, K. Simons, J. Gruenberg, and M. Zerial. 1991. Hypervariable C-terminal domain of rab proteins acts as a targeting signal. *Nature (Lond.).* 353:769–772.
Chavrier, P., R. G. Parton, H. P. Hauri, K. Simons, and M. Zerial. 1990. Localisation of low molecular weight GTP binding proteins to exocytic and endocytic compartments. *Cell.* 62:317–329.
Colombo, M. I., L. S. Mayorga, P. J. Casey, and P. D. Stahl. 1992. Evidence of a role for heterotrimeric GTP-binding proteins in endosome fusion. *Science (Wash. DC).* 255:1695–1697.
Cooper, M. S., A. H. Cornell-Bell, A. Chernjavsky, J. W. Dani, and S. J. Smith. 1990. Tubulovesicular processes emerge from the trans-Golgi cisternae, extend along microtubule, and interlink adjacent trans-Golgi elements into a reticulum. *Cell.* 61:135–145.
Davey, J. S., S. M. Hurtley, and G. Warren. 1985. Reconstitution of an endocytic fusion event in a cell-free system. *Cell.* 43:643–652.
DeBrabander, M., R. Nuydens, H. Geerts, and C. Hopkins. 1988. Dynamic behaviour of the transferrin receptor followed in living epidermoid carcinoma (A431) cells with nanovid microscopy. *Cell Motil. Cytoskeleton.* 9:30–47.
Deng, Y., and B. Storrie. 1988. Animal cell lysosomes rapidly exchange membrane proteins. *Proc. Natl. Acad. Sci. USA.* 85:3860–3864.
Deng, Y. P., G. Griffiths, and B. Storrie. 1991. Comparative behavior of lysosomes and the pre-lysosome compartment (PLC) in in vivo cell fusion experiments. *J. Cell Sci.* 99:571–582.
Diaz, R., L. Mayorga, and P. D. Stahl. 1988. In vitro fusion of endosomes following receptor-mediated endocytosis. *J. Biol. Chem.* 263:6093–6100.
Diaz, R., L. S. Mayorga, P. I. Weidman, J. E. Rothman, and P. D. Stahl. 1989. Vesicle fusion following receptor-mediated endocytosis requires a protein active in Golgi transport. *Nature (Lond.).* 339:398–400.
Dunn, K. A., and F. R. Maxfield. 1992. Delivery of ligands from sorting endosomes to late endosomes occurs by maturation of sorting endosomes. *J. Cell Biol.* 117:301–310.
Emans, N., J.-P. Gorvel, C. Walter, V. Gerke, G. Griffiths, and J. Gruenberg. 1993. Annexin II is a major component of fusogenic endosomal vesicles. *J. Cell Biol.* 120:1357–1370.
Gibbons, I. R., A. Lee-Eiford, G. Mocz, C. A. Philipson, W.-J. Y. Tang, and B. H. Gibbons. 1987. Photosensitized cleavage of dynein heavy chain. Cleavage of the "V1 site" by irradiation at 365 nm in the presence of ATP and vanadate. *J. Biol. Chem.* 262:2780–2786.
Gill, S. R., T. A. Schroer, I. Szilak, E. R. Steuer, M. P. Sheetz, and D. W. Cleveland. 1991. Dynactin, a conserved, ubiquitously expressed component of an activator of vesicle motility mediated by cytoplasmic dynein. *J. Cell Biol.* 115:1639–1650.
Goda, Y., and S. R. Pfeffer. 1989. Cell-free systems to study vesicular transport along the secretory and biosynthetic pathways. *FASEB (Fed. Am. Soc. Exp. Biol.) J.* 3:2488–2494.
Goda, Y., and S. R. Pfeffer. 1991. Identification of a novel N-ethylmaleimide-sensitive cytosolic factor required for vesicular transport from endosomes to the trans-Golgi network in vitro. *J. Cell Biol.* 112:823–831.
Gorvel, J.-P., P. Chavrier, M. Zerial, and J. Gruenberg. 1991. Rab 5 controls early endosome fusion in vitro. *Cell.* 64:915–925.
Griffiths, G., and J. Gruenberg. 1991. The arguments for pre-existing early and late endosomes. *Trends Cell Biol.* 1:5–9.
Griffiths, G., R. Back, and M. Marsh. 1989. A quantitative analysis of the endocytic pathway in baby hamster kidney cells. *J. Cell Biol.* 109:2703–2720.
Griffiths, G., B. Hoflack, K. Simons, I. Mellman, and S. Kornfeld. 1988. The mannose-6-phosphate receptor and the biogenesis of lysosomes. *Cell.* 52:329–341.
Griffiths, G., R. Matteoni, R. Back, and B. Hoflack. 1990. Characterization of the cation-independent mannose-6-phosphate receptor-enriched prelysosomal compartment in NRK cells. *J. Cell Sci.* 95:441–461.
Griffiths, G., A. McDowell, R. Back, and J. Dubochet. 1984. On the preparation of cryosections for immunocytochemistry. *J. Ultrastruct. Res.* 89: 65–78.
Gruenberg, J., and K. E. Howell. 1985. Immuno-isolation of vesicles using antigenic sites either located on the cytoplasmic or the exoplasmic domain of an implanted viral protein. *Eur. J. Cell Biol.* 38:312–321.
Gruenberg, J., and K. E. Howell. 1986. Reconstitution of vesicle fusions occurring in endocytosis with a cell-free system. *EMBO (Eur. Mol. Biol. Organ.) J.* 5:3091–3101.
Gruenberg, J., and K. E. Howell. 1987. An internalized trans-membrane protein resides in a fusion-competent endosome for less than 5 minutes. *Proc. Natl. Acad. Sci. USA.* 84:5758–5762.
Gruenberg, J., and K. E. Howell. 1989. Membrane traffic in endocytosis: insights from cell-free assays. *Annu. Rev. Cell Biol.* 5:453–481.
Gruenberg, J., and M. Clague. 1992. Regulation of intracellular membrane transport. *Curr. Opin. Cell Biol.* 4:593–599.
Gruenberg, J., and J. P. Gorvel. 1992. In vitro reconstitution of endocytic vesicle fusion. *In* Protein Targeting, a Practical Approach. A. I. Magee and T. Wileman, editors. Oxford University Press, Oxford. 187–216.
Gruenberg, J., G. Griffiths, and K. E. Howell. 1989. Characterization of the early endosome and putative endocytic carrier vesicles in vivo and with an assay of vesicle fusion in vitro. *J. Cell Biol.* 108:1301–1316.
Herman, B., and D. F. Albertini. 1984. A time-lapse video image intensification analysis of cytoplasmic organelle movements during endosome translocation. *J. Cell Biol.* 98:565–576.
Hirsch, J. G. 1962. Cinemicrographic observations on granule lysis in polymorphonuclear leucocytes during phagocytosis. *J. Exp. Med.* 116:827–833.
Hollenbeck, P. J., and J. A. Swanson. 1990. Radial extension of macrophage tubular lysosomes supported by kinesin. *Nature (Lond.).* 346:864–866.
Hopkins, C. R., A. Gibson, M. Shipman, and K. Miller. 1990. Movement of internalized ligand-receptor complexes along a continuous endosomal reticulum. *Nature (Lond.).* 346:335–339.
Howell, K. E., R. Schmid, J. Ugelstad, and J. Gruenberg. 1989. Immunoisolation using magnetic solid supports: subcellular fractionation for cell-free functional studies. *Methods Cell Biol.* 31A:264–292.
Ingold, A. L., S. A. Cohn, and J. M. Scholey. 1988. Inhibition of kinesin-driven microtubule motility by monoclonal antibodies to kinesin heavy chains. *J. Cell Biol.* 107:2657–2667.
Kornfeld, S., and I. Mellman. 1989. The biogenesis of lysosomes. *Annu. Rev. Cell Biol.* 5:483–526.
Kreis, T. E. 1986. Micro-injected antibodies against the cytoplasmic domain of vesicular stomatitis virus glycoprotein blocks its transport to the cell surface. *EMBO (Eur. Mol. Biol. Organ.) J.* 5:931–941.
Lee, C., and L. B. Chen. 1988. Dynamic behaviour of endoplasmic reticulum in living cells. *Cell.* 54:37–46.
Lenhard, J. M., R. A. Kahn, and P. D. Stahl. 1992. Evidence for ADP-ribosylation factor (ARF) as a regulator of in vitro endosome-endosome fusion. *J. Biol. Chem.* 267:13047–13052.
Matteoni, R., and T. E. Kreis. 1987. Translocation and clustering of endosomes and lysosomes depends on microtubules. *J. Cell Biol.* 105:1253–1265.
Murphy, R. F. 1991. Maturation models for endosome and lysosome biogenesis. *Trends Cell Biol.* 1:77–82.
Parton, R. G., K. Prydz, M. Bomsel, K. Simons, and G. Griffiths. 1989. Meeting of the apical and basolateral endocytic pathways of the Madin-Darby canine kidney cell in late endosomes. *J. Cell Biol.* 109:3259–3272.
Parton, R. G., K. Simons, and C. G. Dotti. 1992*a*. Axonal and dendritic endocytic pathways in cultured neurons. *J. Cell Biol.* 119:123–137.
Parton, R. G., P. Schrotz, C. Bucci, and J. Gruenberg. 1992*b*. Plasticity of early endosomes. *J. Cell Sci.* 103:335–348.
Paschal, B. M., H. S. Shpetner, and R. B. Vallee. 1987. MAP 1C is a microtubule-activated ATPase which translocates microtubules in vitro and has dynein-like properties. *J. Cell Biol.* 105:1273–1282.
Pastan, I., and W. C. Willingham. 1981. Journey to the center of the cell: role of the receptosome. *Science (Wash. DC).* 214:504–509.
Pfeffer, S. 1992. GTP-binding proteins in intracellular transport. *Trends Cell Biol.* 2:41–46.
Phaire-Washington, L., S. C. Silverstein, and E. Wang. 1980. Phorbol myristate acetate stimulates microtubule and 10-nm filament extension and lysosome redistribution in mouse macrophages. *J. Cell Biol.* 86:641–655.
Pierre, P., J. Schell, J. E. Rickard, and T. E. Kreis. 1992. CLIP-170 links endocytic vesicles to microtubules. *Cell.* 70:887–900.
Rabinowitz, S., H. Horstmann, S. Gordon, and G. Griffiths. 1992. Immunocytochemical characterization of the endocytic and phagolysosomal compartments in peritoneal macrophages. *J. Cell Biol.* 116:95–112.
Rothman, J. E., and L. Orci. 1992. Molecular dissection of the secretory pathway. *Nature (Lond.).* 355:409–415.
Scheel, J., and T. E. Kreis. 1991. Motor protein independent binding of endocytic carrier vesicles to microtubules in vitro. *J. Biol. Chem.* 266:18141–8148.
Schekman, R. 1992. Genetic and biochemical analysis of vesicular traffic in yeast. *Curr. Opin. Cell Biol.* 4:587–592.
Schroer, T. R., B. J. Schnapp, T. S. Reese, and M. P. Sheetz. 1988. The role of kinesin and other soluble factors in organelle movement along microtubules. *J. Cell Sci.* 107:1785–1792.
Schroer, T., E. R. Steuer, and M. P. Sheetz. 1989. Cytoplasmic dynein is a minus-end directed motor for membranous organelles. *Cell.* 56:937–946.
Steuer, E. R., L. Wordeman, T. A. Schroer, and M. P. Sheetz. 1990. Localization of cytoplasmic dynein to mitotic spindles and kinetochores. *Nature (Lond.).* 345:266–268.
Stoorvogel, W., G. J. Strous, H. J. Geuze, V. Oorschot, and A. L. Schwartz.

1991. Late endosomes derive from early endosomes by maturation. *Cell.* 65:417–427.

Swanson, J., A. Bushnell, and S. C. Silverstein. 1987. Tubular lysosome morphology and distribution within macrophages depend on the integrity of cytoplasmic microtubules. *Proc. Natl. Acad. Sci. USA.* 84:1921–1925.

Thomas, L., P. Clarke, M. Pagano, and J. Gruenberg. 1992. Inhibition of membrane fusion in vitro via cyclin B but not cyclin A. *J. Biol. Chem.* 267:6183–6187.

Tuomikoski, T., M. Felix, M. Doree, and J. Gruenberg. 1989. Inhibition of endocytic vesicle fusion in vitro by the cell-cycle control protein kinase cdc2. *Nature (Lond.).* 342:942–945.

Vale, R. D. 1987. Intracellular transport using microtubule-based motors. *Annu. Rev. Cell Biol.* 3:347–378.

Vale, R. D., T. S. Reese, and M. P. Sheetz. 1985. Identification of a novel force-generating protein, kinesin, involved in microtubule-based motility. *Cell.* 42:39–50.

Van der Sluijs, P., M. K. Bennett, C. Antony, K. Simons, and T. E. Kreis. 1990. Binding of exocytic vesicles from MDCK cells to microtubules in vitro. *J. Cell Sci.* 95:545–553.

Vaux, D., J. Tooze, and S. Fuller. 1990. Identification by anti-idiotype antibodies of an intracellular membrane protein that recognizes a mammalian endoplasmic reticulum retention signal. *Nature (Lond.).* 345:495–502.

Woodman, P., D. I. Mundy, P. Cohen, and G. Warren. 1992. Cell-free fusion of endocytic vesicles is regulated by phosphorylation. *J. Cell Biol.* 116: 331–338.

Woodman, P. G., and G. Warren. 1988. Fusion between vesicles from the pathway of receptor-mediated endocytosis in a cell-free system. *Eur. J. Biochem.* 173:101–108.